

Ethanol as fuel additive: high-pressure oxidation of its mixtures with acetylene

*Lorena Marrodán, Miguel Fuster, Ángela Millera, Rafael Bilbao, María U. Alzueta**

Aragón Institute of Engineering Research (I3A). Department of Chemical and Environmental Engineering. University of Zaragoza, Zaragoza-Spain.

ABSTRACT

An experimental and modeling study of the oxidation of acetylene-ethanol mixtures under high-pressure conditions (10-40 bar) has been carried out in the 575-1075 K temperature range, in a plug flow reactor. The influence on the oxidation process of the oxygen inlet concentration (determined by the air excess ratio, λ) and the amount of ethanol (0-200 ppm) present in the reactant mixture has also been evaluated. In general, the predictions obtained with the proposed model are in satisfactory agreement with the experimental data. For a given pressure, the onset temperature for acetylene conversion is almost the same independently of the oxygen or ethanol concentrations in the reactant mixture, but it is shifted to lower temperatures when the pressure is increased. Under the conditions of this study, the ethanol presence does not modify the main reaction routes for acetylene conversion, being its main effect the modification of the radical pool composition.

INTRODUCTION

Fuel reformulation seems to be a promising strategy for minimizing important pollutants emitted to the atmosphere during combustion processes, especially from transportation, such as nitrogen oxides (NO_x) and soot, the principal component of particulate matter. Government regulations are becoming stricter, there is an increasing global warming concern and fossil fuel resources are finite. Therefore, the bio-derived oxygenated fuels and fuel additives are paid more attention in the last years and awaken the research community interest, as shown by Kohse-Höinghaus et al. [1] when reviewing biofuel combustion chemistry.

Among all possible biofuels, ethanol is one of the most common biofuels and it has been widely studied and used, either directly or as a gasoline additive. However, its application in diesel engines is restricted because its cetane number, flash point and calorific values are lower compared to diesel fuel. For this reason, ethanol must be blended with diesel or biodiesel to overcome all these difficulties. In this way, regarding to the exhaust pollutant emissions, although there is certain controversy about if it is possible to reduce simultaneously CO, soot or nitrogen oxides emissions, authors such as An et al. [2] indicate that, working under given conditions, for example at comparatively lower temperatures, soot and nitrogen oxides emissions could be reduced by using ethanol. This controversy makes necessary a systematic study at laboratory scale under well controlled operating conditions in order to acquire a better knowledge of the possible effects of the ethanol addition to fuel.

In recent years, the role of ethanol as additive to diesel or gasoline has been studied in engines [e.g. 3, 4], and when added to different hydrocarbons (such as acetylene, ethylene, n-heptane, propene, iso-octane or benzene, among others) in laboratory flames [for example, 5-9], jet-stirred

1
2
3 reactors (JSR) [10-11] and plug flow reactors [12], to investigate its influence on combustion
4 performance and pollutant emissions. Dagaut and Togbé [10] carried out an experimental and
5 modeling study of the oxidation of different mixtures of iso-octane with ethanol and 1-butanol in
6 JSR, at an equivalence ratio of 1, and a pressure of 10 atm, with a good agreement between
7 experimental and modeling calculations. Reaction rate analyses showed that the reaction paths
8 were very similar when increasing the alcohol fraction in the mixture. In a similar way, Rezgui
9 and Guemini [11] carried out a computational study, based on the experimental results
10 previously obtained by Ristori et al. [13] and Aboussi [14], of the effects of ethanol addition on
11 the formation of some pollutants during benzene JSR oxidation and their results indicated that
12 the mole fractions of acetylene (C_2H_2), cyclopentadienyl radical (C_5H_5) and propargyl radical
13 (C_3H_3) decreased when increasing the ethanol percentage in the mixture. In an atmospheric plug
14 flow reactor, Abián et al. [12] analyzed the effect of temperature (775-1375 K), air excess ratio
15 (from fuel-rich to fuel-lean conditions) and the ethanol concentration (0-200 ppm) on the
16 oxidation of acetylene-ethanol mixtures. They stated that the main reaction pathways observed
17 for acetylene conversion in the presence of ethanol were basically the same as those in its
18 absence, and the influence of ethanol addition comes from its capacity to modify the composition
19 of the radical pool. Moreover, Esarte et al. [15] analyzed soot formation from the pyrolysis of
20 acetylene, ethanol and their mixtures, and the results showed that adding small concentrations of
21 ethanol (600 times lower than acetylene concentration) leads to a diminution on the production
22 of soot from acetylene pyrolysis.

23
24
25
26
27
28
29
30
31
32
33
34
35
36
37
38
39
40
41
42
43
44
45
46
47
48
49
50 However, despite its relevance for its applicability to internal combustion engines, and the
51 current tendency in designing combustion systems working at high-pressure to increase
52
53
54
55
56
57
58
59
60

1
2
3 efficiency, to our knowledge, no experimental or modeling studies have been carried out
4
5 evaluating the impact of ethanol addition to hydrocarbons at pressures higher than 10 atm.
6
7

8
9 In this context, the aim of the present work is to study the high-pressure oxidation of acetylene-
10 ethanol mixtures, which will extend the experimental database on the behavior of ethanol as
11 additive. Therefore, the oxidation of acetylene-ethanol mixtures in a quartz flow reactor under
12 high-pressure conditions has been studied from both experimental and modeling points of view.
13
14 Acetylene (C_2H_2) has been set as the main fuel because it is recognized as one of the main soot
15 precursors, it is an important intermediate in combustion of hydrocarbons, and a recent chemical
16 kinetic mechanism for modeling its conversion under high-pressure conditions is available [16].
17
18 The experimental results obtained have been used to validate a chemical kinetic mechanism able
19 to describe the oxidation of both compounds and their mixtures under the conditions studied.
20
21 This will extend the applicability of the model to other operating conditions and it can be used as
22 a predicting tool.
23
24
25
26
27
28
29
30
31
32
33
34
35
36
37

38 EXPERIMENTAL SECTION

39
40
41 The experiments have been carried out in a laboratory-scale high-pressure flow reactor designed
42 to approximate plug-flow [17], which has been described elsewhere [18], and therefore only the
43 most relevant details are mentioned here. The oxidation of C_2H_2 (approximately 500 ppm) and
44 ethanol (C_2H_5OH , 0-200 ppm) mixtures has been analyzed in the 575-1075 K temperature range.
45
46 To evaluate the influence of pressure on the oxidation process, different manometric pressures
47 have been tested, 10-40 bar. The oxygen inlet concentration has been varied from reducing to
48 oxidizing conditions by modifying the value of lambda ($\lambda=0.7$, 1 and 20), defined as the inlet
49
50
51
52
53
54
55
56
57
58
59
60

1
2
3 oxygen divided by the stoichiometric oxygen, and considering both fuel components, acetylene
4 and ethanol. Nitrogen is used to balance up to obtain a total gas flow rate of 1 L (STP)/min.
5
6
7 Reactants are highly diluted minimizing the reaction thermal effects. Reactant gases, supplied
8
9
10 from gas cylinders, are premixed before entering the reactor. Table 1 lists the conditions for the
11
12 different experiments.
13

14
15 The oxidation reactions take place in a tubular quartz tube (inner diameter of 6 mm and 1500
16
17 mm in length) enclosed in a steel pressure shell and placed in an electrically heated oven. Type K
18
19 thermocouples, positioned in the void between the quartz reactor and the steel shell, were used to
20
21 measure the longitudinal temperature profiles, obtaining an isothermal reaction zone (± 10 K) of
22
23 56 cm. The temperature profiles, for 10 and 40 bar, can be found as Supporting Information
24
25 (Figure S1 and S2, respectively). The gas residence time in the isothermal zone can be
26
27 represented by $t_r(\text{s}) = 261 P(\text{bar})/T(\text{K})$, which implies that residence time depends on both
28
29 pressure and temperature. Downstream of the reactor, the pressure of the system is reduced to
30
31 atmospheric level before product analysis, which is performed using a micro-gas chromatograph
32
33 (Agilent 3000A) equipped with Thermal Conductivity Detectors (TCD), and an ATI Mattson
34
35 Fourier Transform Infrared spectrometer. The uncertainty of measurements is estimated as $\pm 5\%$,
36
37
38 except for the FTIR spectrometer, which is estimated as $\pm 10\%$. The atomic carbon balance was
39
40
41 checked, and the deviations were below 10% in most of the cases.
42
43
44
45
46
47
48
49

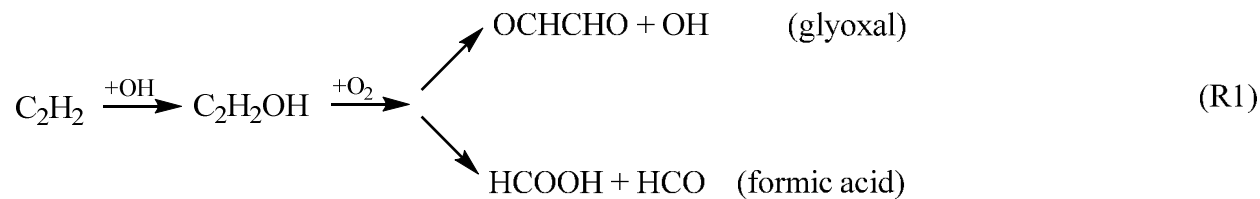
50 CHEMICAL KINETIC MODEL

51
52
53
54
55
56
57
58
59
60

1
2
3 The experimental results have been analyzed in terms of a detailed gas-phase chemical kinetic
4 mechanism for chemistry description and analysis of the oxidation under high-pressure
5 conditions of C₂H₂-C₂H₅OH mixtures.
6
7
8
9

10
11 The mechanism, as well as the thermodynamic data, proposed by our group to describe the
12 ethanol high-pressure oxidation [19] have been taken in the present work without any
13 modifications. This mechanism includes the reaction subset for ethanol conversion suggested by
14 Alzueta and Hernández [20]. Calculations coincide, in general, well with the main experimental
15 trends observed. Other mechanisms in literature are available. As an example, we have tested a
16 very recent mechanism by Hashemi et al. [21], proposed to describe the pyrolysis and oxidation
17 of ethanol under high-pressure conditions. The results indicate that modeling predictions are also
18 in good agreement with the experimental trends observed in the present work (Figures S3-S5, in
19 Supporting Information).
20
21
22
23
24
25
26
27
28
29
30

31
32 The present mechanism takes as a basis the GADM mechanism [22], progressively updated (e.g.
33 [23, 24]) and modified to consider the high-pressure conditions and the different compounds
34 involved [17, 25-27]. The reaction subset proposed by Giménez-López et al. [16] for oxidation
35 of acetylene at intermediate temperatures and high pressure, was also included. These authors
36 indicated that through the sequence represented in (R1) significant amounts of glyoxal and
37 formic acid may be formed from acetylene. Therefore, the reaction subsets for these compounds
38 (refs. [28] and [29], respectively) were also added to the present mechanism.
39
40
41
42
43
44
45
46
47
48
49
50
51
52
53
54
55
56
57
58
59
60



Although no special implication of compounds such as methyl formate, dimethoxymethane or dimethyl ether is expected, the present mechanism also includes reaction subsets for these compounds, which have been validated under high-pressure conditions ([18], [30] and [31], respectively). We found that some reactions involving HCOOH proposed by Zhao et al. [32], slightly improve present model calculations. Most of these reactions (Table S1, in Supporting Information) are H abstraction and decomposition reactions which occur in only one step (e.g. $\text{HCOOH} + \text{OH} = \text{H}_2\text{O} + \text{CO}_2 + \text{H}$), whereas in the formic acid subset by Marshall and Glarborg [29], this is produced in two steps: a H abstraction (e.g. $\text{HCOOH} + \text{OH} = \text{HOCO} + \text{H}_2\text{O}$), followed by the decomposition of the hydrocarboxyl radical produced (e.g. $\text{HOCO} + \text{M} = \text{CO} + \text{OH} + \text{M}$). Examples of the discrepancies obtained in modeling calculations with or without these reactions, for conditions denoted as sets 1-4 in Table 1, are given in Supporting Information (Figures S6-S9). The influence of these reactions, although low, indicates an uncertainty in the behavior of HCOOH and, therefore, an effort should be made in better understanding its oxidation.

The mechanism obtained by this way involves 137 species and contains 798 reactions, and as mentioned above, it is the same successfully used in a high-pressure ethanol oxidation study [19]. The complete mechanism and the thermodynamic data are provided as Supporting Information.

1
2
3 Numerical calculations were conducted with the plug-flow reactor module of CHEMKIN-PRO
4 software package [33] and considering the corresponding temperature profiles determined
5 experimentally.
6
7
8
9

10 11 12 13 14 RESULTS AND DISCUSSION 15

16
17 The oxidation of C₂H₂-C₂H₅OH mixtures has been studied in the 575-1075 K temperature range.
18 In addition to temperature, the influence of the pressure (10 and 40 bar), the air excess ratio (λ)
19 and the concentration of ethanol in the mixture (0-200 ppm) has been analyzed from both
20 experimental and modeling points of view. Figure 1 shows an example of the results for the
21 consumption with temperature of the reactants C₂H₂, C₂H₅OH, and oxygen, and for the
22 formation of different products quantified (CO, CO₂, H₂ and CH₃CHO), for the conditions
23 denoted as set 2 in Table 1. From now on, experimental results are denoted by symbols whereas
24 model calculations are denoted by lines. In general, there is a good agreement between
25 experimental and modeling results. Moreover, all the experimental results obtained in the present
26 work can be found in an excel spreadsheet as Supporting Information.
27
28
29
30
31
32
33
34
35
36
37
38
39
40

41 Figures 2 and 3 show the evolution with temperature of C₂H₂, C₂H₅OH, CO and CO₂
42 concentrations for stoichiometric conditions ($\lambda=1$), 10 bar and different inlet ethanol
43 concentrations. Apparently, under the present high-pressure conditions, neither the presence nor
44 the amount of ethanol do modify significantly the onset temperature for acetylene oxidation nor
45 the acetylene conversion profile, in contrast to what was observed by Abián et al. [12] in their
46 atmospheric pressure oxidation work of C₂H₂-C₂H₅OH mixtures ($t_r(s)=195/T(K)$, 500 ppm of
47 C₂H₂ and 0-200 ppm of C₂H₅OH). In that study, as the amount of ethanol was increased, the
48
49
50
51
52
53
54
55
56
57
58
59
60

1
2
3 acetylene conversion occurred at higher temperatures. Under the present high-pressure
4 conditions (10 bar), the oxidation of C_2H_2 starts at 775-800 K approximately, independently of
5 the amount of ethanol present in the reactant mixture. In the case of ethanol, it also starts to be
6 consumed at the same temperature as C_2H_2 , that is, 775-800 K approximately, and independently
7 of the amount added to the mixture; whereas under atmospheric conditions [12], ethanol was
8 more reactive being completely consumed at lower temperatures than acetylene, and once
9 ethanol was consumed, C_2H_2 concentration sharply decayed.

10
11
12 On the other hand, for the lower amounts of ethanol, 0 and 50 ppm, the modeling predictions for
13 CO and CO_2 seem to be in good agreement with the experimental data. However, for higher
14 amounts of ethanol, the CO concentration is underpredicted by the model, whereas, the
15 concentration of CO_2 is overestimated. This indicates that, although the experimental trends of
16 both compounds are well predicted by the model, further work could be done to improve
17 modeling predictions in the oxidation pathways of C_2H_2 and C_2H_5OH to CO and CO_2 . At
18 present, we are not able to clearly identify what is the reason for the poor fitting of the
19 calculations versus experimental individual data of CO and CO_2 . However, the sum of both CO
20 and CO_2 is well described by calculations (bottom part of Figure 3). Since the reaction rate of the
21 conversion of CO into CO_2 is known with certain confidence, the differences may be attributed
22 to inexactitudes in predicting the H/O radical pool composition, which may arise from a number
23 of reactions involved in the mechanism feeding the radical pool.

24
25
26 To evaluate the influence of the oxygen availability in the reactant mixture on the oxidation of
27 the mixtures, different air excess ratios (λ) have been used for two different ethanol
28 concentrations in the mixture, 50 or 200 ppm, while keeping constant the value of the pressure at
29 10 bar and the C_2H_2 concentration (500 ppm, approximately). The experimental results obtained

1
2
3 for acetylene and ethanol consumption and CO formation, as one of the major oxidation
4 products, are compared with modeling calculations and represented in Figure 4. The inlet oxygen
5 concentration does not significantly modify the acetylene, neither for the lowest concentration of
6 ethanol in the mixture (50 ppm, left part of Figure 4) nor for the highest (200 ppm, right part of
7 Figure 4). The temperature for the onset of C₂H₂ oxidation, and therefore, the onset of CO
8 formation is almost independent of the value of lambda analyzed. In the case of ethanol, as it was
9 previously reported in a high-pressure (20, 40 and 60 bar) ethanol oxidation study [19], for a
10 given pressure, the inlet oxygen concentration does not clearly modify the C₂H₅OH oxidation,
11 and ethanol is completely consumed for all the stoichiometries analyzed. One possible
12 explanation to the almost negligible effect of the oxygen availability on the onset temperature for
13 ethanol consumption could be that ethanol oxidation is initiated by its thermal dehydration to
14 ethylene (reaction R2) and its thermal decomposition through bond cleavage to CH₂OH and CH₃
15 radicals (reaction R3) [19].
16
17
18
19
20
21
22
23
24
25
26
27
28
29
30
31
32
33



40
41 Another study of the oxidation of C₂H₂-C₂H₅OH mixtures, but under atmospheric pressure
42 conditions [12], also indicates that the onset temperature of acetylene and ethanol conversion is
43 almost the same (around 900 K) for all the values of lambda analyzed, but the temperature range
44 for full consumption of acetylene and ethanol was different depending on the value of lambda
45 analyzed, unlike what is observed at high-pressure. Thus, at atmospheric pressure and the leanest
46 conditions studied ($\lambda=20$), the full conversion of acetylene was produced at approximately 100 K
47
48
49
50
51
52
53
54
55
56
57
58
59
60

1
2
3 below compared to $\lambda=0.7$ and stoichiometric conditions ($\lambda=1$), while for $\lambda=0.2$, C_2H_2 was not
4 completely consumed even for the highest temperature analyzed in that study, 1375 K.
5
6

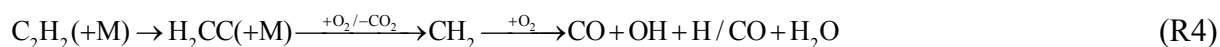
7
8
9 The influence of a change in the working pressure (from 10 to 40 bar) on the oxidation of C_2H_2 -
10 C_2H_5OH mixtures has also been evaluated (Figure 5). As listed in Table 1, for ethanol
11 concentrations in the mixture of 50 and 200 ppm, the three different values of lambda have been
12 tested for both pressures, although not all of them have been represented in Figure 5. As
13 previously mentioned, the impact of the inlet oxygen on the C_2H_2 - C_2H_5OH mixtures oxidation is
14 almost negligible.
15
16
17
18
19
20
21
22

23
24 As it can be seen in Figure 5, an increase in working pressure appears to shift the onset of C_2H_2
25 oxidation to lower temperatures, approximately 50-75 K. Therefore, the conversion of C_2H_2 at 40
26 bar starts at 725 K, which is approximately the same temperature to that obtained under similar
27 experimental conditions by Giménez-López et al. [16] in their high-pressure (60 bar) oxidation
28 study of C_2H_2 (total flow rate of 3 L(STP)/min, residence times of 10-15 s in the isothermal
29 reaction zone). Therefore, a change in pressure from 10 to 40 bar has significant effects on the
30 conversion of C_2H_2 and C_2H_5OH , but the effects are less pronounced when pressure is further
31 increased.
32
33
34
35
36
37
38
39
40
41

42
43 Since the model provides good performance when simulating the oxidation of C_2H_2 - C_2H_5OH
44 mixtures, model calculations at different pressures were run to compare modeling predictions for
45 C_2H_2 consumption for different pressures, stoichiometric conditions and for approximately 50
46 ppm of ethanol. The results obtained from this theoretical evaluation are shown in Figure 6. As it
47 can be seen, the most significant changes occur in the 1-10 pressure range. As described in the
48 Experimental Section, the residence time of the gas in the isothermal zone, can be represented by
49
50
51
52
53
54
55
56
57
58
59
60

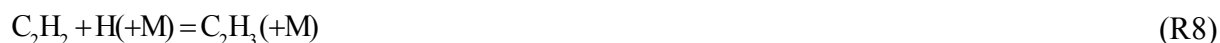
1
2
3 t_r (s)=261 P(bar)/T(K). So, when pressure is increased from 1 to 10 bar, the residence time is also
4
5 increased by a factor of 10, in addition to the increase in species concentration by increasing the
6
7 system pressure. As a consequence, the onset temperature changes steeply. In the same way, a
8
9 change from 10 to 20 bar implies an increase in the residence time of 2 and from 60 to 100 bar,
10
11 an increase of 1.7 times, and the effect in the onset temperature is less pronounced in the last
12
13 case. Additionally, an experiment at 20 bar, which is within the pressure range object of this
14
15 study, has been performed under similar conditions (set 5 in Table 1). As it can be seen, the
16
17 present mechanism is able to reproduce again the trend experimentally observed, strengthening
18
19 the reliability of the present mechanism.
20
21
22
23
24

25 In general, model predictions reproduce the experimental observations. Therefore, with the
26
27 present mechanism, a reaction rate analysis has been performed which has allowed to identify
28
29 the main routes for C₂H₂ and C₂H₅OH consumption and products formation during the oxidation
30
31 of C₂H₂-C₂H₅OH mixtures. A diagram with the main reaction pathways is represented in Figure
32
33 7. The width of the arrows and the values included in the figure correspond to the percentage of
34
35 consumption of the corresponding compound, for the conditions and reactor distance indicated in
36
37 its caption. In the case of acetylene, its conversion is initiated through the sequence described in
38
39 (R4) and reactions with O₂ such as reaction (R5) to form HCO, which may react with oxygen
40
41 producing HO₂ radicals and more CO (R6). Upon initiation, C₂H₂ undergoes addition reactions
42
43 generating intermediate adducts, that is, C₂H₂ reacts with OH radicals to produce the CHCHOH
44
45 adduct (R7), which is the main acetylene consumption route independently of the value of the air
46
47 excess ratio analyzed, but it becomes more relevant as the oxygen availability increases.
48
49
50
51
52





The C_2H_2 combination with H radicals to form vinyl radicals (C_2H_3), reaction (R8), is important under stoichiometric ($\lambda=1$) and, especially, for fuel-rich conditions ($\lambda=0.7$). Reactions of C_2H_2 with O radicals (R9 and R10) are of less importance compared to the previous one. For example, under the same conditions described in the caption of Figure 7, i.e. 800 K, and the experimental conditions denoted as set 3 in Table 1 (10 bar, $\lambda=1$ and 42 ppm of ethanol in the blend), reaction (R8) represents a 20% whereas (R9 and R10) only a 6% of the total C_2H_2 consumption.



Although, the CHCHOH adduct could decompose thermally or react with O/H radicals, under the conditions of this work, it mainly reacts with O_2 to form formic acid, HCOOH (R11). Giménez-López et al. [16] indicated that glyoxal (OCHCHO) could also be formed in considerable concentration from reaction of the CHCHOH adduct with O_2 , but, under the present conditions, this route is almost negligible.



The slight discrepancies in model calculations related to HCOOH reactions from Zhao et al. [32], mentioned in the Chemical Kinetic Model section, do not modify the mentioned reaction routes. It only changes the way in which formic acid is converted, that is, directly to CO and CO₂ (reactions R12 and R13) or through HOCO and OCHO (R14), which later decompose to produce CO and CO₂.



In conclusion, acetylene is mainly consumed following the sequence: $\text{C}_2\text{H}_2 + \text{OH} \rightarrow \text{CHCHOH} \xrightarrow{+\text{O}_2} \text{HCOOH} \rightarrow \text{CO}, \text{CO}_2$, independently of the value of lambda. However, in a previous study of the oxidation of C₂H₂-C₂H₅OH mixtures at atmospheric pressure [12], although the possible reaction routes were almost the same, the predominant ones were those involving interactions of C₂H₂ and H and O radicals.

The reaction routes for C₂H₂ above described are almost the same than those described in a high-pressure acetylene oxidation work [16], only with differences under reducing conditions. In that work, C₂H₂ was mostly consumed by recombination with H to form vinyl radicals. However, under the present conditions, C₂H₂ is mainly consumed by reaction with OH radicals under all the stoichiometries analyzed. So, apparently, under the present conditions, the addition of ethanol to the reactant mixture does not modify the acetylene oxidation regime. It only modifies the composition of the radical pool, increasing the relevance of C₂H₂ reactions with OH radicals. Therefore, the effectiveness of ethanol in reducing soot formation from acetylene, that has been

proved in different works (e.g. [15]), is probably produced by the oxygen present in ethanol which contributes to an increase of the O/OH radical pool, therefore favoring C₂H₂ oxidation towards CO and CO₂ and hence, removing carbon from the reaction paths which lead to soot formation.

On the other hand, ethanol conversion is initiated by its thermal dehydration to ethylene and water (R15). The water generated may react with O₂ (R16) or with H radicals (R17) generated from the oxidation of C₂H₂ (for example, in reaction R5) and, therefore, HO₂ and OH radicals are formed.

After initiation, C₂H₅OH is mainly consumed by H abstraction reactions leading to the formation of three different ethanol radicals (CH₃CHOH, CH₂CH₂OH or CH₃CH₂O), depending on the site where the H abstraction occurs [19] (represented in reaction R18, where R can be O, H, OH, CH₃ or HO₂ radicals).



The abstraction of hydrogen from ethanol by HO₂ radicals is very important in the initial steps of ethanol consumption, but as OH radicals are generated, this becomes the more relevant oxidation route. As represented in Figure 7, a 41% of the ethanol conversion occurs through H abstraction by OH radicals to form CH₃CH₂O (R19) and a 27% occurs also through H abstraction by OH

radicals to form the other ethanol radical, CH₃CHOH (R20). The third option of H abstraction reaction from ethanol by OH radicals is to produce the CH₂CH₂OH radical (R21), but it less relevant compared to the other routes (15%). Previous ethanol oxidation works, under high and atmospheric pressure conditions [19, 20], indicate that the CH₂CH₂OH radical may react with O₂ to form formaldehyde (R22). Under the present conditions, this radical reacts with H₂O₂ (- R23) to give back ethanol due to the high concentration of H₂O₂ under high-pressure conditions (HO₂ + HO₂ = H₂O₂ + O₂). Oxygen is preferably consumed in other routes than in R22.



The ethanol radicals, CH₃CHOH and CH₃CH₂O, react with O₂ or just decompose thermally (R24 and R25, respectively), to form acetaldehyde (CH₃CHO), or in the case of CH₃CH₂O, it can also decompose and produce CH₃ radicals and formaldehyde (R26).



1
2
3 The reaction routes for ethanol, described above and represented in Figure 7, are the most
4 relevant ones under the conditions of this work and they are almost the same than those
5 previously described in earlier studies concerning the oxidation of ethanol or its mixtures [12,
6
7
8
9
10 19].

11
12
13 Therefore, it seems that during the joint oxidation of ethanol and acetylene, there is no direct
14 interaction between both compounds; each of them follows their corresponding reaction routes,
15 and their oxidation is only modified by an increase in the O/OH radical pool generated during the
16 conversion of the other reactant.
17
18
19
20
21
22

23 Moreover, a first-order sensitivity analysis for CO has been performed for the conditions denoted
24 as sets 2-4, 6-8 and 11-13 in Table 1, in the very beginning of the C₂H₂-C₂H₅OH mixtures
25 conversion; it means when the concentration of CO is around 10 ppm. The results obtained,
26 shown in Table 2, indicate the most sensitive reactions for the different values of lambda (λ=0.7,
27 1 and 20), pressures (10 and 40 bar) and concentrations of ethanol (50 or 200 ppm) in the blend.
28 In general, the normalized sensitivity coefficients obtained for all the conditions analyzed are
29 very similar, indicating that there is not a huge difference between the coefficients if lambda,
30 pressure and/or the amount of ethanol are changed. In the case of acetylene, its reaction with
31 HO₂ radicals (R27) is very sensitive due to the OH radicals generated which interact with
32 acetylene and ethanol (R7 and R18, respectively).
33
34
35
36
37
38
39
40
41
42
43
44
45
46



48
49
50
51 To our knowledge, there is no direct determination for the rate constant of reaction (R27). The
52 temperature and pressure dependent rate coefficients, together with the whole reaction subset for
53 C₂H₂, as mentioned in the Chemical Kinetic Model section, have been adopted from the recent
54
55
56
57
58
59
60

1
2
3 work on high-pressure acetylene oxidation by Giménez-López et al. [16]. The authors stated that
4 $C_2H_2+HO_2$ reaction involves nine different pressure and temperature dependent product
5 channels, with the formation of CHCHO being the dominant under the studied conditions. In that
6 paper, it is also indicated that the rate constant for these reactions had not been previously
7 determined experimentally, and only a room temperature upper limit of $3 \times 10^9 \text{ cm}^3 \text{ mol}^{-1} \text{ s}^{-1}$ was
8 available in literature [34]. Therefore, and considering the similarities between the $C_2H_3O_2$
9 potential energy diagrams (PES) relative to $C_2H_2+HO_2$ and $C_2H_3+O_2$ systems, Giménez-López et
10 al. [16] adopted the temperature and pressure dependent rate coefficients for these reactions from
11 the $C_2H_3+O_2$ kinetic analysis by Goldsmith et al. [35]. A better determination of this reaction rate
12 would be though desirable.
13
14
15
16
17
18
19
20
21
22
23
24
25

26
27 On the other hand, in the case of ethanol, two H abstraction reactions to form CH_2CH_2OH and
28 CH_3CHOH radicals, appear among the most sensitive reactions (Table 2). The coefficients
29 obtained for the first reaction are negative, OH radicals are removed from the main oxidation
30 pathways; whereas, the H abstraction from ethanol by HO_2 radicals is promoting, the ethanol
31 radical generated in this case is more reactive, and the H_2O_2 also produced decomposes
32 generating very reactive OH radicals.
33
34
35
36
37
38
39
40

41
42 As mentioned before, although some uncertainties in modeling calculations related to HCOOH
43 reactions were found, none of these reactions appeared among the most sensitive ones, so they
44 do not have a significant influence on the results.
45
46
47
48
49
50

51 52 53 CONCLUSIONS 54 55 56 57 58 59 60

1
2
3 The influence of temperature (575-1075 K), pressure (10 or 40 bar), inlet oxygen concentration
4 ($\lambda=0.7$, 1 or 20) and concentration of ethanol in the reactant mixture (50-200 ppm) has been
5
6 evaluated in the high-pressure oxidation of acetylene-ethanol mixtures. The detailed chemical
7
8 kinetic mechanism previously compiled by our group in a high-pressure ethanol oxidation work
9
10 [19] has been used in this work for calculations. In general, the mechanism is able to reproduce
11
12 the wide range of conditions experimentally tested. Neither the oxygen concentration nor the
13
14 amount of ethanol added to the reaction mixture have a significant influence on the onset
15
16 temperature for the conversion of C_2H_2 . Only an increase in pressure (when moving from 10 to
17
18 40 bar) shifts the onset for acetylene conversion to lower temperatures. The reaction routes for
19
20 acetylene consumption remain practically unaltered by the addition of ethanol in comparison to
21
22 those obtained in the high-pressure oxidation study of acetylene [16], being the C_2H_2 interaction
23
24 with OH radicals the main consumption route for the lambdas analyzed. Apparently, there is no
25
26 interaction between acetylene and ethanol; their respective oxidation is only modified by an
27
28 increase in the O/OH radical pool produced during the conversion of the other reactant.
29
30
31
32
33
34
35
36
37
38
39

40 ASSOCIATED CONTENT

41 42 **Supporting Information**

43
44
45 The Supporting Information is available free of charge on the ACS Publications website.
46
47
48
49
50

51 AUTHOR INFORMATION

52 53 **Corresponding Author**

1
2
3 *E-mail: uxue@unizar.es
4
5

6 **Notes**

7
8
9 The authors declare no competing financial interest.
10
11
12
13

14 **ACKNOWLEDGMENTS**

15
16
17 The authors express their gratitude to Aragón Government and European Social Fund (GPT
18 group), and to MINECO and FEDER (Project CTQ2015-65226) for financial support. Ms.
19 Marrodán acknowledges Aragón Government for the predoctoral grant awarded.
20
21
22
23
24
25

26 **REFERENCES**

- 27
28
29
30 [1] Kohse-Höinghaus, K.; Oßwald, P.; Cool, T.A.; Kasper, T.; Hansen, N.; Qi, F.; Westbrook,
31 C.K.; Westmoreland, P.R. Biofuel combustion chemistry: from ethanol to biodiesel. *Angew.*
32 *Chem. Int. Ed.* 2010, 49, 3572-3597.
33
34
35
36
37
38 [2] An, H.; Yang, W.M.; Li, J. Effects of ethanol addition on biodiesel combustion: a modeling
39 study. *Appl. Energy* 2015, 143, 176-188.
40
41
42
43 [3] Alptekin, E. Evaluation of ethanol and isopropanol as additives with diesel fuel in a CRDI
44 diesel engine. *Fuel* 2017, 205, 161-172.
45
46
47
48
49 [4] Sakai, S.; Rothamer, D. Effect of ethanol blending on particulate formation from premixed
50 combustion in spark-ignition engines. *Fuel* 2017, 196, 154-168.
51
52
53
54
55
56
57
58
59
60

- 1
2
3 [5] Bierkandt, T.; Kasper, T.; Akyildiz, E.; Lucassen, A.; Oßwald, P.; Köhler, M.; Hemberger, P.
4
5 Flame structure of a low-pressure laminar premixed and lightly sooting acetylene flame and the
6
7 effect of ethanol addition. *Proc. Combust. Inst.* 2015, 35, 803-811.
8
9
10
11 [6] Bennett, B.A.V; McEnally, C.S.; Pfefferle, L.D.; Smooke, M.D.; Colket, M.B.
12
13 Computational and experimental study of the effects of adding dimethyl ether and ethanol to
14
15 nonpremixed ethylene/air flames. *Combust. Flame* 2009, 156, 1289-1302.
16
17
18
19 [7] Inal, F.; Senkan, S.M. Effects of oxygenate concentration on species mole fractions in
20
21 premixed n-heptane flames. *Fuel* 2005, 84, 495-503.
22
23
24
25 [8] Kohse-Höinghaus, K.; Oßwald, P.; Struckmeier, U.; Kasper, T.; Hansen, N.; Taatjes C.A.;
26
27 Wang, J.; Cool, T.A.; Gon, S.; Westmoreland, P.R. The influence of ethanol addition on
28
29 preximed fuel-rich propene-oxygen-argon flames. *Proc. Combust. Inst.* 2007, 31, 1119-1127.
30
31
32
33 [9] Dong, L. Detailed influences of ethanol as fuel additive on combustion chemistry of
34
35 premixed fuel-rich ethylene flames. *Sci. China Tech. Sci.* 2015, 58, 1696-1704.
36
37
38
39 [10] Dagaut, P.; Togbé, C. Oxidation kinetics of mixtures of iso-octane with ethanol or butanol
40
41 in a jet-stirred reactor: experimental and modeling study. *Combust. Sci. Technol.* 2012, 184,
42
43 1025-1038.
44
45
46 [11] Rezgui, Y.; Guemini M. Effect of ethanol on soot precursors emissions during benzene
47
48 oxidation in a jet-stirred reactor. *Environ. Sci. Pollut. Res.* 2014, 21, 6671-6686.
49
50
51
52 [12] Abián, M.; Esarte, C.; Millera, Á.; Bilbao, R.; Alzueta, M.U. Oxidation of acetylene-ethanol
53
54 mixtures and their interaction with NO. *Energy Fuel* 2008, 22, 3814-3823.
55
56
57
58
59
60

- 1
2
3 [13] Ristori, A.; Dagaut, P.; El Bakali, A.; Pengloan, G; Cathonnet, M. Benzene oxidation:
4 experimental results in a JSR and comprehensive kinetic modeling in JSR, shock-tube and flame.
5
6
7
8 *Combust. Sci. Tech.* 2001, 167, 223-256.
9
10
11 [14] Aboussi, B. Etude expérimentale et modélisation de l'oxydation de l'éthanol. *PhD Thesis*,
12 1991, University of Orleans.
13
14
15
16 [15] Esarte, C.; Callejas, A.; Millera, Á.; Bilbao, R.; Alzueta, M.U. Influence of the
17 concentration of ethanol and the interaction of compounds in the pyrolysis of acetylene and
18 ethanol mixtures. *Fuel* 2011, 90, 844-849.
19
20
21
22
23
24 [16] Giménez-López, J.; Rasmussen, C.T.; Hashemi, H.; Alzueta, M.U.; Gao, Y.; Marshall, P.;
25 Goldsmith, F.; Glarborg, P. Experimental and kinetic modeling study of C₂H₂ oxidation at high
26 pressure. *Int. J. Chem. Kinet.* 2016, 48, 724-738.
27
28
29
30
31
32 [17] Rasmussen, C.L.; Hansen, J.; Marshall, P.; Glarborg, P. Experimental measurements and
33 kinetic modeling of CO/H₂/O₂/NO_x conversion at high pressure. *Int. J. Chem. Kinet.* 2008, 40,
34 454-480.
35
36
37
38
39
40 [18] Marrodán, L.; Millera, Á.; Bilbao, R.; Alzueta, M.U. High-pressure study of methyl formate
41 oxidation and its interaction with NO. *Energy Fuels* 2014, 28, 6107-6115.
42
43
44
45
46 [19] Marrodán, L.; Arnal, Á.J.; Millera, Á.; Bilbao, R.; Alzueta, M.U. High-pressure ethanol
47 oxidation and its interaction with NO. *Fuel* 2018, 223, 394-400.
48
49
50
51 [20] Alzueta, M.U.; Hernández, J.M. Ethanol oxidation and its interaction with nitric oxide.
52
53
54 *Energy Fuels* 2002, 16, 166-171.
55
56
57
58
59
60

1
2
3 [21] Hashemi, H.; Christensen, J.M.; Glarborg, P. High-pressure pyrolysis and oxidation of
4 ethanol. *Fuel* 2018, 218, 247-257.
5
6

7
8 [22] Glarborg, P.; Alzueta, M.U.; Dam-Johansen, K.; Miller, J.A. Kinetic modeling of
9 hydrocarbon/nitric oxide interactions in a flow reactor. *Combust. Flame* 1998, 115, 1-27.
10
11

12
13 [23] Glarborg, P.; Alzueta, M.U.; Kærsgaard, K.; Dam-Johansen, K. Oxidation of formaldehyde
14 and its interaction with nitric oxide in a flow reactor. *Combust. Flame* 2003, 132, 629-638.
15
16

17
18 [24] Glarborg, P.; Østberg, M.; Alzueta, M.U.; Dam-Johansen, K.; Miller, J.A. The
19 recombination of hydrogen atoms with nitric oxide at high temperatures. *Proc. Combust. Inst.*
20 1999, 27, 219-227.
21
22

23
24 [25] Rasmussen, C.L.; Glarborg, P. Measurements and kinetic modeling of CH₄/O₂ and
25 CH₄/C₂H₆/O₂ conversion at high-pressure. *Int. J. Chem. Kinet.* 2008, 40, 778-807.
26
27

28
29 [26] Rasmussen, C.L.; Andersen, K.H.; Dam-Johansen, K.; Glarborg, P. Methanol oxidation in a
30 flow reactor: implications for the branching ratio of CH₃OH+OH reaction. *Int. J. Chem. Kinet.*
31 2008, 40, 423-441.
32
33

34
35 [27] Rasmussen, C.L.; Glarborg, P. Sensitizing effects of NO_x on CH₄ oxidation at high pressure.
36 *Combust. Flame* 2008, 154, 529-545.
37
38

39
40 [28] Faßheber, N.; Friedrichs, G.; Marshall, P.; Glarborg, P. Glyoxal oxidation mechanism:
41 implications for the reactions HCO+O₂ and OCHCHO+HO₂. *J. Phys. Chem. A* 2015, 119, 7305-
42 7315.
43
44
45
46
47
48
49
50
51
52
53
54
55
56
57
58
59
60

1
2
3 [29] Marshall, P.; Glarborg, P. Ab initio and kinetic modeling studies of formic acid oxidation.
4
5 *Proc. Combust. Inst.* 2015, 35, 153-160.
6

7
8 [30] Marrodán, L.; Royo, E.; Millera, Á.; Bilbao, R.; Alzueta, M.U. High pressure oxidation of
9
10 dimethoxymethane. *Energy Fuels* 2015, 29, 3507-3517.
11
12

13
14 [31] Marrodán, L.; Arnal, Á.J.; Millera, Á.; Bilbao, R.; Alzueta, M.U. The inhibiting effect of
15
16 NO addition on dimethyl ether high-pressure oxidation. Submitted.
17
18

19
20 [32] Zhao, Z.; Chaos, M.; Kazakov, A.; Dryer, F.L. Thermal decomposition reaction and a
21
22 comprehensive kinetic model of dimethyl ether. *Int. J. Chem. Kin.* 2008, 40, 1-18.
23
24

25 [33] ANSYS Chemkin-Pro 17.2; Reaction Design: San Diego, 2016.
26
27

28
29 [34] Bohn, B.; Zetsch, C.J. Formation of HO₂ from OH and C₂H₂ in the presence of O₂. *J.*
30
31 *Chem. Soc., Faraday Trans.* 1998, 94, 1203-1210.
32
33

34 [35] Goldsmith, C.F.; Harding, L.B.; Georgievskii, Y.; Miller, J.A.; Klippenstein, S.J.
35
36 Temperature and pressure-dependent rate coefficients for the reaction of vinyl radical with
37
38 molecular oxygen. *J. Phys. Chem. A.* 2015, 119, 7766-7779.
39
40
41
42
43
44
45
46
47
48
49
50
51
52
53
54
55
56
57
58
59
60

1
2
3 **Table captions**
4
5

6 **Table 1.** Matrix of experimental conditions. Experiments are conducted in the 575-1075 K
7 temperature range. The balance is closed with N₂.
8

9 **Table 2.** Normalized sensitivity coefficients for CO for sets 2-4, 6-8 and 11-13 in Table 1^(a).
10
11
12
13
14
15
16
17
18
19
20
21
22
23
24
25
26
27
28
29
30
31
32
33
34
35
36
37
38
39
40
41
42
43
44
45
46
47
48
49
50
51
52
53
54
55
56
57
58
59
60

Table 1. Matrix of experimental conditions. Experiments are conducted in the 575-1075 K temperature range. The balance is closed with N₂.

Set	C ₂ H ₂ [ppm]	C ₂ H ₅ OH [ppm]	P [bar]	λ
1	569	-	10	1
2	467	49	10	0.7
3	537	42		1
4	424	46		20
5	544	52	20	1
6	490	51	40	0.7
7	566	48		1
8	565	50		20
9	574	96	10	1
10	559	140	10	1
11	552	170	10	0.7
12	531	242		1
13	420	210		20
14	554	210	40	0.7
15	575	204		1
16	551	211		20

Table 2. Normalized sensitivity coefficients for CO for sets 2-4, 6-8 and 11-13 in Table 1^(a).

reaction	Set 2 775 K	Set 3 775 K	Set 4 775 K	Set 6 700 K	Set 7 700 K	Set 8 700 K	Set 11 775 K	Set 12 775 K	Set 13 775 K
$\text{HO}_2+\text{HO}_2=\text{H}_2\text{O}_2+\text{O}_2$	-0.81	-0.83	-0.78	-1.01	-1.02	-1.02	-0.84	-0.85	-0.81
$\text{H}_2\text{O}_2(+\text{M})=\text{OH}+\text{OH}(+\text{M})$	0.70	0.72	0.73	0.78	0.78	0.81	0.80	0.85	0.85
$\text{CH}_2+\text{O}_2=\text{CO}+\text{H}_2\text{O}$	-0.14	-0.13	-0.14	-0.07	-0.07	-0.07	-0.11	-0.10	-0.11
$\text{CH}_2+\text{O}_2=\text{CO}_2+\text{H}+\text{H}$	0.05	0.05	0.05	0.03	0.03	0.03	0.04	0.04	0.05
$\text{CH}_2+\text{O}_2=\text{CH}_2\text{O}+\text{O}$	0.04	0.04	0.05	0.02	0.02	0.03	0.03	0.03	0.04
$\text{C}_2\text{H}_2(+\text{M})=\text{H}_2\text{CC}(+\text{M})$	0.01	0.01	0.08	0.00	0.00	0.02	0.01	0.01	0.09
$\text{C}_2\text{H}_2+\text{O}=\text{HCCO}+\text{H}$	0.26	0.26	0.21	0.19	0.19	0.18	0.21	0.18	0.14
$\text{C}_2\text{H}_2+\text{O}=\text{CH}_2+\text{CO}$	-0.26	-0.25	-0.21	-0.19	-0.19	-0.18	-0.19	-0.15	-0.12
$\text{C}_2\text{H}_2+\text{OH}=\text{CHCHOH}$	0.21	0.18	0.22	0.15	0.13	0.11	0.36	0.39	0.43
$\text{C}_2\text{H}_2+\text{HO}_2=\text{CH}_2\text{CHOO}$	-0.02	-0.02	-0.01	-0.06	-0.05	-0.05	-0.02	-0.01	-0.01
$\text{C}_2\text{H}_2+\text{HO}_2=\text{CHCHO}+\text{OH}$	2.16	2.14	1.87	1.89	1.92	1.87	1.81	1.64	1.42
$\text{H}_2\text{CC}+\text{O}_2=\text{CH}_2+\text{CO}_2$	0.08	0.07	0.04	0.02	0.01	0.02	0.07	0.07	0.03
$\text{C}_2\text{H}_5\text{OH}+\text{OH}=\text{CH}_2\text{CH}_2\text{OH}+\text{H}_2\text{O}$	-0.11	-0.09	-0.10	-0.07	-0.06	-0.06	-0.22	-0.26	-0.26
$\text{C}_2\text{H}_5\text{OH}+\text{HO}_2=\text{CH}_3\text{CHOH}+\text{H}_2\text{O}_2$	0.22	0.17	0.23	0.26	0.23	0.25	0.53	0.68	0.69

^(a) The normalized sensitivity coefficients are given as $A_i\delta Y_j/Y_j\delta A_i$, where A_i is the pre-exponential constant for reaction i and Y_j is the mass fraction of j_{th} species. Therefore, the sensitivity coefficients listed can be interpreted as the relative change in predicted concentration for the species j caused by increasing the rate constant for reaction i by a factor of 2.

Figure captions

Figure 1. Evolution of C_2H_2 , C_2H_5OH , O_2 , CO , CO_2 , H_2 and CH_3CHO concentrations with temperature during the high-pressure (10 bar) oxidation of C_2H_2 - C_2H_5OH mixtures, for the conditions denoted as set 2 in Table 1.

Figure 2. Influence of the amount of ethanol added to the mixture on the concentration profiles of C_2H_2 and C_2H_5OH during the C_2H_2 - C_2H_5OH mixtures oxidation, as a function of temperature, for stoichiometric conditions ($\lambda=1$) and 10 bar. Experimental results are denoted by symbols and modeling calculations by lines. The inlet conditions correspond to sets 1, 3, 9, 10 and 12 in Table 1.

Figure 3. Influence of the amount of ethanol added to the mixture on the concentration profiles of CO , CO_2 and the sum of both during the C_2H_2 - C_2H_5OH mixtures oxidation, as a function of temperature, for stoichiometric conditions ($\lambda=1$) and 10 bar. Experimental results are denoted by symbols and modeling calculations by lines. The inlet conditions correspond to sets 1, 3, 9, 10 and 12 in Table 1.

Figure 4. Influence of the air excess ratio (λ) on the concentration profiles of C_2H_2 and CO (upper part) and C_2H_5OH (lower part) during the C_2H_2 - C_2H_5OH mixtures oxidation, as a function of temperature, for 10 bar and two different amounts of ethanol added to the blend, 50 ppm (left part) and 200 ppm (right part). Experimental results are denoted by symbols and modeling calculations by lines. The inlet conditions correspond to sets 2-4 and 11-13 in Table 1.

Figure 5. Influence of pressure on the concentration profiles of C_2H_2 , C_2H_5OH and CO during the C_2H_2 - C_2H_5OH mixtures oxidation, as a function of temperature and for different values of the air excess ratio. Experimental results are denoted by symbols and modeling calculations by lines. The inlet conditions correspond to sets 3, 6-8, 12 and 15 in Table 1.

Figure 6. Evaluation through model calculations of the pressure effect on temperature evolution of C_2H_2 concentration predicted by the model for a mixture of C_2H_2 and C_2H_5OH and stoichiometric conditions ($\lambda=1$).

Figure 7. Main reaction pathways for C_2H_2 (left) and C_2H_5OH (right) consumption and product formation. The percentages in the diagram corresponds to 800 K, and the experimental conditions denoted as set 3 in Table 1. The selected position in the reactor is 105 cm, it corresponds to the point at which the concentration of C_2H_2 is about 470 ppm and the C_2H_5OH concentration, 34 ppm.

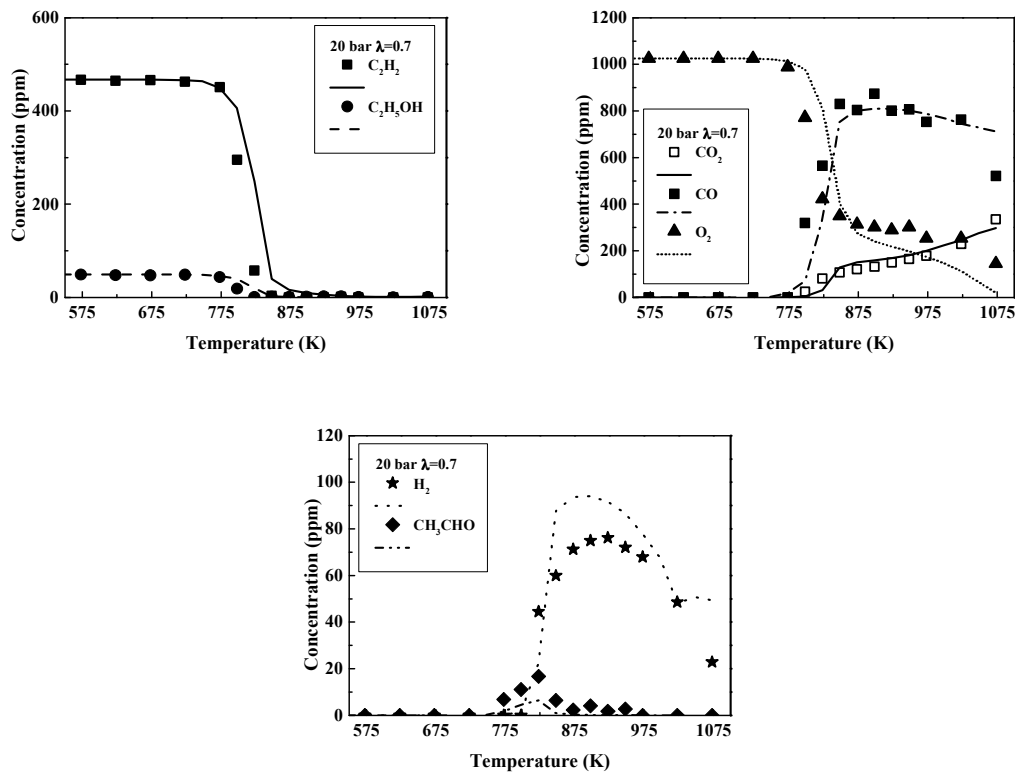


Figure 1. Evolution of C₂H₂, C₂H₅OH, O₂, CO, CO₂, H₂ and CH₃CHO concentrations with temperature during the high-pressure (10 bar) oxidation of C₂H₂-C₂H₅OH mixtures, for the conditions denoted as set 2 in Table 1.

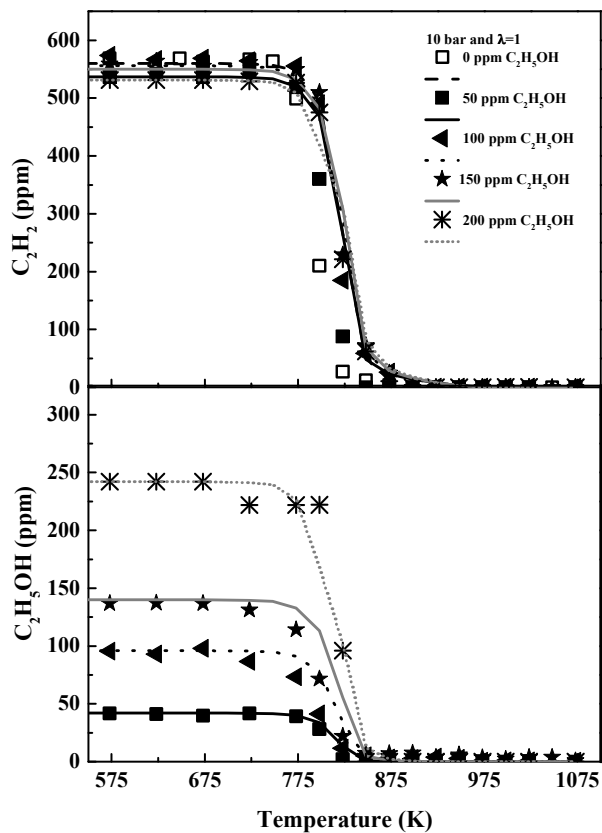


Figure 2. Influence of the amount of ethanol added to the mixture on the concentration profiles of C₂H₂ and C₂H₅OH during the C₂H₂-C₂H₅OH mixtures oxidation, as a function of temperature, for stoichiometric conditions ($\lambda=1$) and 10 bar. Experimental results are denoted by symbols and modeling calculations by lines. The inlet conditions correspond to sets 1, 3, 9, 10 and 12 in

Table 1.

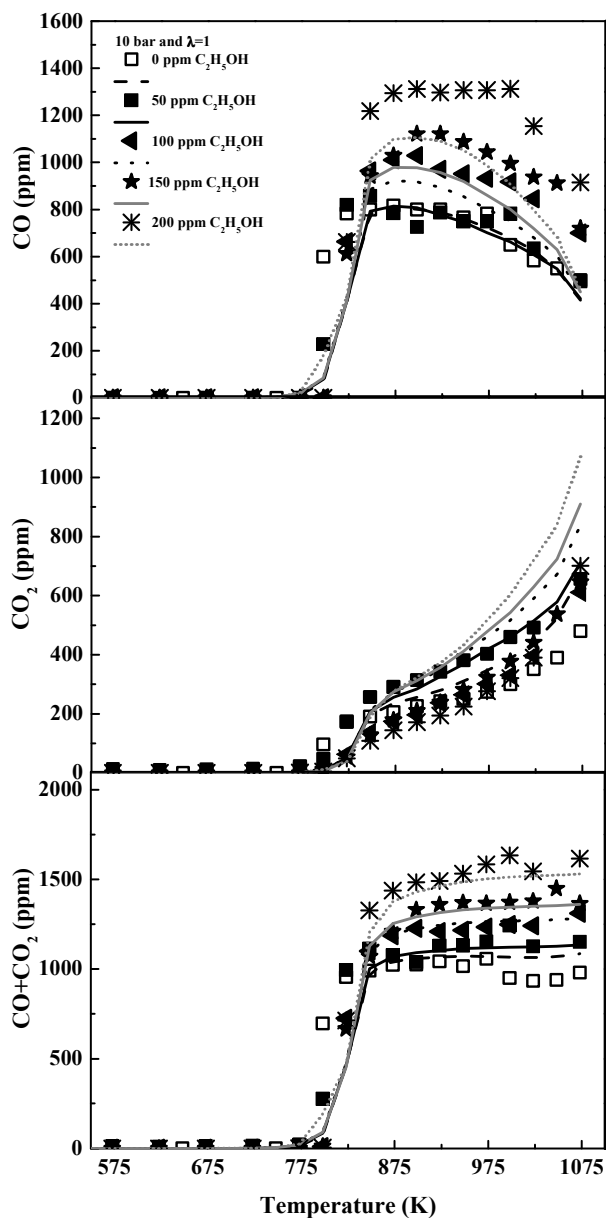


Figure 3. Influence of the amount of ethanol added to the mixture on the concentration profiles of CO, CO₂ and the sum of both during the C₂H₂-C₂H₅OH mixtures oxidation, as a function of temperature, for stoichiometric conditions ($\lambda=1$) and 10 bar. Experimental results are denoted by symbols and modeling calculations by lines. The inlet conditions correspond to sets 1, 3, 9, 10 and 12 in Table 1.

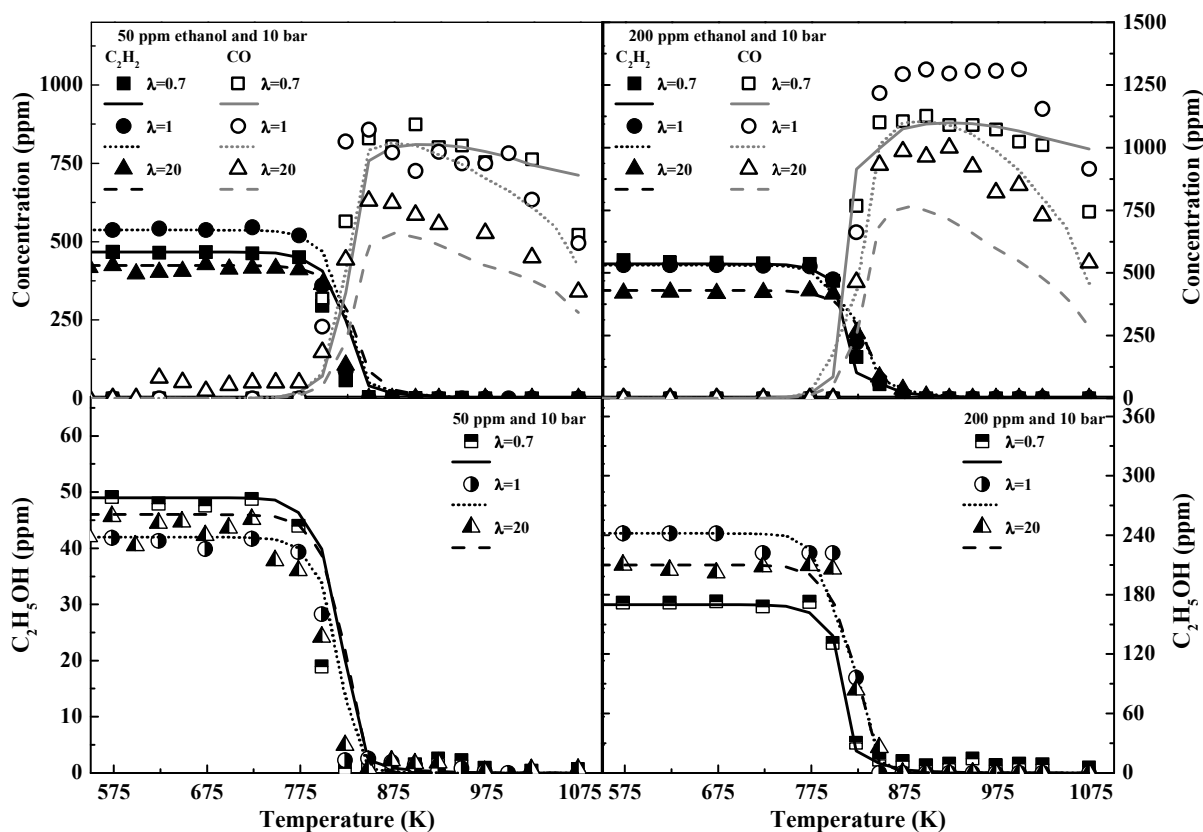


Figure 4. Influence of the air excess ratio (λ) on the concentration profiles of C₂H₂ and CO (upper part) and C₂H₅OH (lower part) during the C₂H₂-C₂H₅OH mixtures oxidation, as a function of temperature, for 10 bar and two different amounts of ethanol added to the blend, 50 ppm (left part) and 200 ppm (right part). Experimental results are denoted by symbols and modeling calculations by lines. The inlet conditions correspond to sets 2-4 and 11-13 in Table 1.

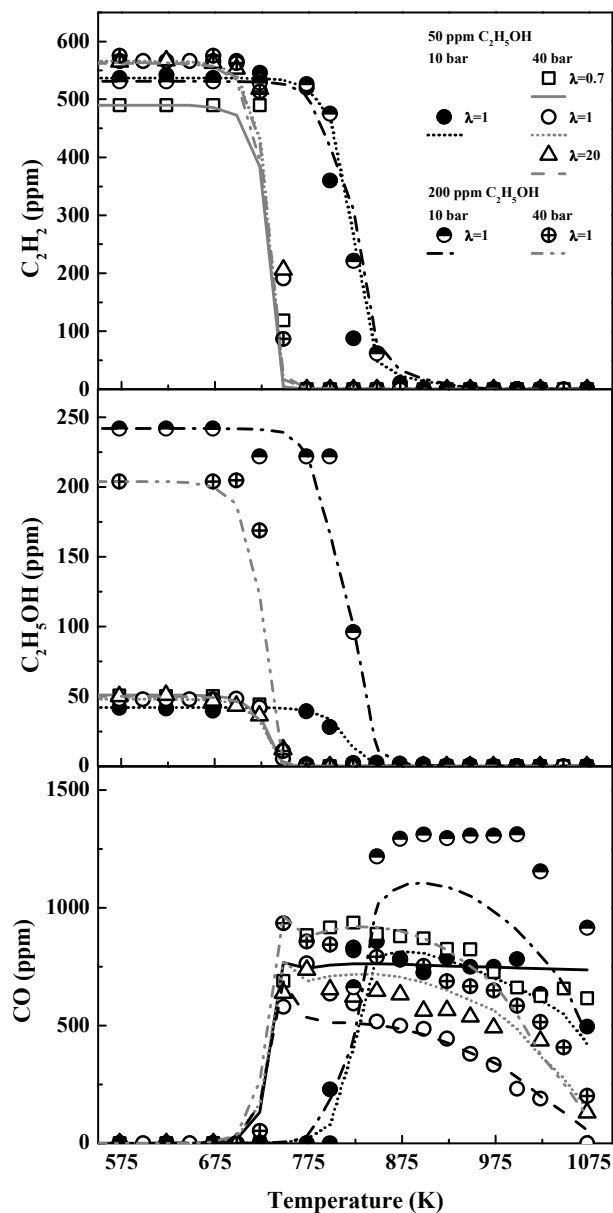


Figure 5. Influence of pressure on the concentration profiles of C_2H_2 , C_2H_5OH and CO during the C_2H_2 - C_2H_5OH mixtures oxidation, as a function of temperature and for different values of the air excess ratio. Experimental results are denoted by symbols and modeling calculations by lines. The inlet conditions correspond to sets 3, 6-8, 12 and 15 in Table 1.

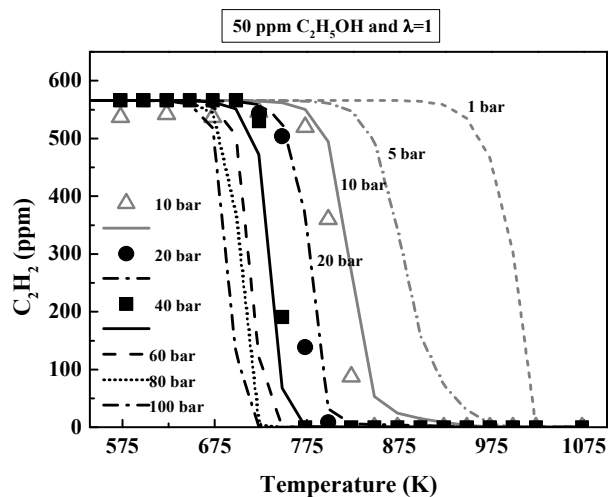


Figure 6. Evaluation through model calculations of the pressure effect on temperature evolution of C_2H_2 concentration predicted by the model for a mixture of C_2H_2 and C_2H_5OH and stoichiometric conditions ($\lambda=1$).

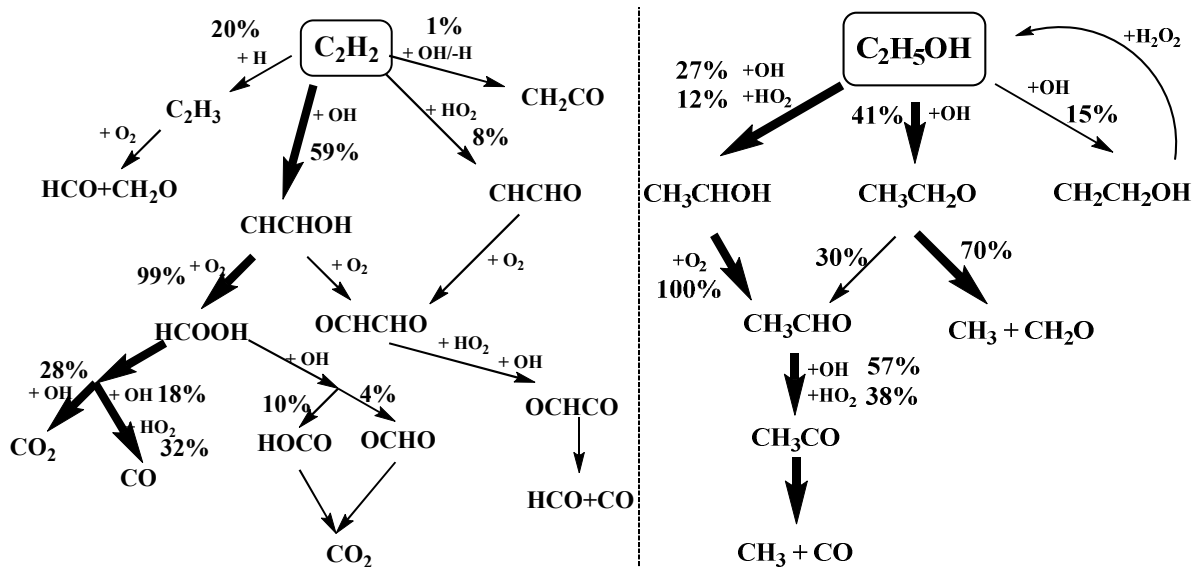


Figure 7. Main reaction pathways for C_2H_2 (left) and C_2H_5OH (right) consumption and product formation. The percentages in the diagram corresponds to 800 K, and the experimental conditions denoted as set 3 in Table 1. The selected position in the reactor is 105 cm, it corresponds to the point at which the concentration of C_2H_2 is about 470 ppm and the C_2H_5OH concentration, 34 ppm.